Towards a DER-Centered Resilient Power System: Testbed Design and Grid Diagnosis

Shirin Besati*, Robert Cox*†, Badrul Chowdhury*†, Ehab Shoubaki*†, and Miao Wang*†

* Department of Electrical and Computer Engineering, University of North Carolina at Charlotte, Charlotte, USA
† Energy Production & Infrastructure Center, University of North Carolina at Charlotte, Charlotte, USA
Email: * { $sbesati$, $robert.cox$, $b.chowdhury$, $eshoubak$, $miao.wang$}@charlotte.edu

***Abstract*—To achieve a carbon-neutral society, future power grids will depend on high penetrations of Distributed Energy Resources (DERs), including solar panels, battery storage, and Electric Vehicles (EVs), which increases the complexity of whole-system dynamics and motivates the need for DER-centered cyber-physical resilience. Few works provide high-fidelity transmission and distribution (T&D) co-simulation that captures time-synchronized interactions under increasing DER integration at large-scale. This paper develops a T&D co-simulation platform that integrates multiple DERs and demonstrates its application through an EV-focused use case by establishing an EV charging aggregator with software-controlled chargers to avoid feeder overloading. Using dynamic EV charging demands and co-simulation feedback, we design a coordinated spatio-temporal strategy for fast EV charging and discharging while respecting operational limits in the power system. Numerical results show that the proposed approach reduces feeder peak coincidence and improves EV charging performance without violating grid constraints.**

***Index Terms*—Smart grid; distributed energy resources (DERs); high-fidelity transmission–distribution co-simulation; electric vehicle (EV) charging**

I. Introduction

To achieve a carbon-neutral society, future power grids are expected to be dependent on a high penetration of variable resources such as renewable distributed energy resources (DERs), which may include solar panels, EVs, battery Energy storage Systems (BESS) [1]. For example, due to increasing environmental concerns caused by petroleum combustion, EVs, powered by electric batteries, will become critical components of future transportation systems, reducing greenhouse gas emissions from the transportation sectors [2], [3].

With the increasing penetration of DERs in the future grid, it is challenging to coordinate and control millions of consumer-type connected DERs in the future cyber-physical power systems. In literature, the distribution systems were analyzed without sufficient consideration of the dynamics, leading to inaccurate representations of real-world system behaviors of DERs. Furthermore, dynamic grid-forming inverter models (GFMs) were not adequately considered in the existing literature. These models are essential for analyzing the behaviors and impacts of inverter-based resources on the grid, particularly in scenarios with high penetration levels. Last but not least, transmission and distribution were usually studied separately in the traditional power system, with presumptions to represent the dynamics of each other at the interconnected boundary. However, the dynamics of modern power systems with the integration of DERs have brought more challenges to the traditional model [4], [5]. The boundary between transmission and distribution operations is now increasingly blurred, which makes co-simulation integrating Transmission and Distribution (T&D) necessary [6]. Furthermore, considering the wide area distribution and high intermittency of DERs, modeling the interaction of renewable energy with the bulk power transmission system in T&D co-simulation at scale is highly computationally intensive. Hence, high-performance computing (HPC)-based T&D co-simulation testbeds are desired but it is challenging to provide accurate and fast computation in response to urgent demands [7].

Thanks to GridLAB-D and GridPACK developed by Pacific Northwest National Laboratory (PNNL) [8], [9], within the T&D co-simulation we built a DER aggregator virtualization platform with software-controlled DER devices that supports grid diagnosis and recovery services in a dynamic and rapid manner. On top of these software-controlled capabilities, the EV aggregator employs as the coordinator that, using co-simulation feedback, computes a spatio-temporal charge/discharge schedule with the aim of reducing feeder–peak coincidence, maintain secure operation within grid limits, and meet charging requirements within the testbed. The contributions of this work are three-fold.

- We design DER-centered, HPC-based T&D co-simulation testbeds for resilient power system studies, emulating transmission, storage, consumption tracking, communication, coordination, and control; the testbeds provide real life dynamic context and massive scaling for modeling DER-centered cyber-physical grids, including DER inverters and flexible loads (e.g., solar panels and EVs).
- A spatio-temporal coordinated DER management is developed and integrated into the co-simulation workflow, which conducts the coordinated EV charging/discharging schedules under feeder limits, station availability, and SoC dynamics.
- We validate the approach in co-simulation, showing reduced feeder–peak coincidence and improved adherence to feeder constraints, demonstrating the benefits of coordinated EV scheduling.

The remainder of the paper is organized as follows. Section

979-8-3315-8138-1

II summarizes recent studies in T&D co-simulation. Section III depicts the architecture of co-simulation. Sections IV and V present the system models and the proposed EV charging strategy design. Section VI provides the numerical results. Section VII concludes the paper.

II. Related Works

Several studies have proposed methods for improving power flow accuracy in integrated transmission and distribution systems with high penetration of DERs. Bharati and Ajjarapu [10] examined the influence of distribution-connected DGs on transmission voltage stability. Khan et al. [11] compared decoupled and unified solutions for coupled networks, highlighting trade-offs in accuracy and efficiency. These works demonstrate that even in steady-state environments, detailed modeling of distribution systems can significantly affect transmission-level outcomes, particularly under high variability from DERs. Moreover, to develop dynamic co-simulation frameworks between T&D systems, Rezvani et al. [12] presented a simulation environment incorporating DER models to assess interactions between distribution-connected IBRs and bulk systems. Although these studies demonstrate the value of time-synchronized dynamics, many platforms are still limited in scale or in handling bidirectional feedback between domains.

Thanks to scalable co-simulation platforms like HELICS [13], integration across simulation domains, such as GridLAB-D and GridPACK, can be enabled, due to its federated time management and support for distributed execution. This feature makes it a key enabler for modern T&D co-simulation, highlighting the novelty of our work compared to existing solutions in the literature.

III. Architecture of Co-simulation

The proposed co-simulation integrates transmission, distribution, and transportation systems. Collected data includes real-time traffic traces from the transportation system, utility demands at distribution buses, and DG energy supplies that mitigate EV-induced grid impacts.

A. Framework of Co-simulation

Fig. 1 shows the co-simulation framework, composing of transportation system, transmission and distribution systems in power grid. The transportation system is simulated from real trace files to capture EV mobility, charging demand, and traffic condition nearby charging stations. The charging stations are connected to distribution nodes. The estimated charging demands at stations are passed to the power system at each timestep via HELICS from transportation simulator.

B. Power System Simulation

The power system is modeled with the IEEE 145-bus transmission network in GridPACK and the IEEE 123-bus three-phase unbalanced distribution system in GridLAB-D. These models have been widely used by researchers to study the performance of distribution grids [14]. The interface (through HELICS) between simulators ensures synchronized time-steps and consistent information exchange across simulation.

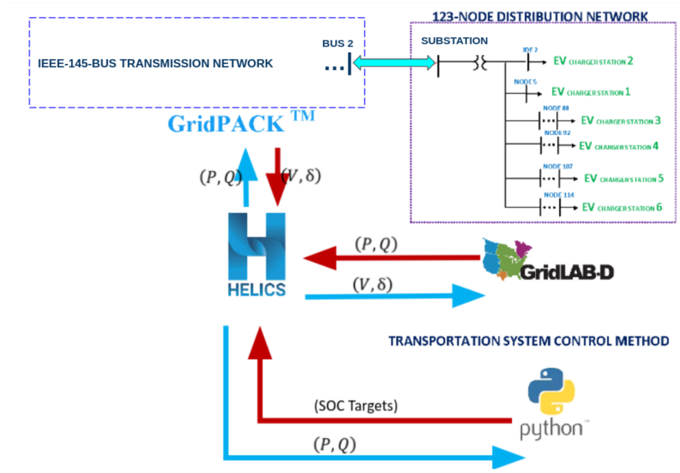

Fig. 1: Co-Simulation Architecture

The control algorithms applied in the simulation to validate the system performance in the real time manner. As shown in Fig. 1, GridLAB-D interacts with 145-bus transmission system through HELICS. GridLAB-D publishes three-phase power signals to GridPACK, while GridLAB-D receives three-phase voltages from GridPACK. HELICS interfaces facilitate data exchange, enabling simulated parameters such as active and reactive power to be seamlessly transferred between T&D systems.

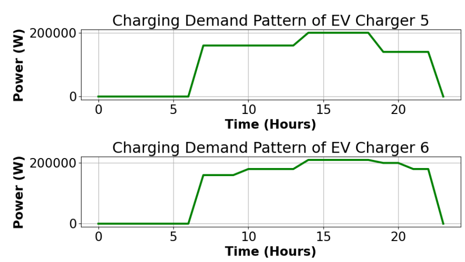

Fig. 2: Scheduled charging profiles of EVCS 5 and EVCS 6 over a 24-hour period.

IV. System Models

We consider the IEEE 145-bus transmission system and IEEE 123-bus distribution system in this work. Let N denote the number of distribution buses (123 buses) that contain PV nodes, battery resources, residential loads, and charging stations. Φ is defined as the set of phases in the three-phase model, where phase $\varphi \in \Phi$. Time T is divided into time steps, e.g., each step is 20 minutes. we deliberately denote the EV charging stations by CS to reflect this paper's focus on transportation-integrated T&D grids, where EVs may charge or discharge at buses in Ω^{CS}. In time step t, the charging or discharging power at bus i in phase φ is $p_{i,t,\varphi}^{CS}$, where $i \in \Omega^{CS}$ and $\varphi \in \Phi$. To maintain power balance and minimize losses, the reference power at bus i is denoted $P_{i,t,\varphi}^{CS,ref}$. M is the set of EVs in the region, with a penetration rate of 5%. The charging load of the a^{th} EV ($a \in M$) at station i in phase

979-8-3315-8138-1

φ at time t is $p^{CS}_{a,i,t,\varphi}$. If $p^{CS}_{a,i,t,\varphi} \geq 0$, EV a is charging; if $p^{CS}_{a,i,t,\varphi} \leq 0$, EV a is discharging. The real and reactive power injections at bus i in the network are established by the AC power flow equations (1)–(2), ensuring that the defined power variables are physically consistent with the network model.

$$P_{i,t} = V_{i,t} \sum_{j=1}^{N} V_{j,t} (G_{ij} \cos\phi_{ij,t} + B_{ij} \sin\phi_{ij,t}), \quad (1)$$

$$Q_{i,t} = V_{i,t} \sum_{j=1}^{N} V_{j,t} (G_{ij} \sin\phi_{ij,t} - B_{ij} \cos\phi_{ij,t}), \quad (2)$$

where $P_{i,t}$, $Q_{i,t}$ are active and reactive power injections at bus i; $V_{i,t}$ and $\varphi_{i,t}$ are the voltage magnitude and phase angle at bus i; G_{ij} and B_{ij} are elements of the bus admittance matrix, and $\phi_{ij,t}$ is the difference between the voltage phase angles at bus i and bus j at time t. Each bus voltage magnitude must remain within operational limits:

$$V^{\min}_{i,t} \leq V_{i,t} \leq V^{\max}_{i,t}, \quad \forall i \in N, \forall t \quad (3)$$

These fundamental grid equations and constraints provide a solid foundation for the coordinated EV charging operations within the power system.

V. Problem Formulation and EV Charging Strategy Design

We coordinate EV charging using information from both the transportation and power systems. Within the GridLAB-D distribution model, EV charging stations (EVCSs) are explicitly modeled as controllable agents that adjust their power in response to GridPACK commands derived from power-flow analysis with bus-voltage limits. To quantify tracking performance, we use a station–level reference and a convex objective. The optimization is carried out subject to the physical and operational constraints below, which define the feasible set and are enforced at each time step within the centralized convex quadratic program. Specifically, station operation is bounded by (i) EVCS power limits in Eq. (4), (ii) feeder capacity in Eq. (5):

$$p^{\mathrm{CS}}_{i,t,\varphi} \leq P^{\mathrm{CS,ref}}_{i,t,\varphi}, \qquad \forall t, i, \quad (4)$$

$$P^{\mathrm{base}}_t + \sum_i p^{\mathrm{CS}}_{i,t,\varphi} \leq \overline{P}^{\mathrm{feed}}_t, \qquad \forall t, \quad (5)$$

where $P^{\mathrm{base}}_t \in \mathbb{R}$ is the base (non-EV) feeder load at time t; and $\overline{P}^{\mathrm{feed}} \in \mathbb{R}$ is the feeder capacity. Since the station-level setpoints are satisfied, we improve realism and accuracy by incorporating transportation system information into the subsequent equations of the optimization model. The charging and discharging constraints per EV in Eq. (6) is defined to ensure that the aggregate station decision remains feasible under individual vehicle limits. Each EV a at station i is subject to individual bounds on charging and discharging power:

$$\overline{P}^{\mathrm{EV,V2G}} \leq p^{CS}_{a,i,t,\varphi} \leq \overline{P}^{\mathrm{EV}}, \qquad \forall t, a, i, \varphi. \quad (6)$$

The parameter $\overline{P}^{\mathrm{EV}}$ is the maximum per-EV charging power, while $\overline{P}^{\mathrm{EV,V2G}}$ is the maximum per-EV discharging power. By having Eq. (6), the power balance of the station is enforced in Eq. (7), where the net station power equals the aggregate EV contributions.

$$p^{\mathrm{CS}}_{i,t,\varphi} = \sum_{a\in\mathcal{A}} A_{t,a,i}\, p^{\mathrm{CS}}_{a,i,t,\varphi}, \qquad \forall t, i, \varphi, \quad (7a)$$

$$\sum_i A_{t,a,i} \leq 1, \qquad \forall t, a. \quad (7b)$$

The binary indicator $A_{t,a,i} \in \{0, 1\}$ specifies whether EV a is connected and available to charge/discharge at station $i \in \Omega^{CS}$ at time t. Eq. (7b) determines each EV is uniquely assigned to a single charging station at any given time. Furthermore, tracking each vehicle's State of Charge (SoC) is essential; accordingly, the SoC of each electric vehicle ($E_{t,a}$) with its initial amount ($E^{\mathrm{Init}}_{a,t}$) evolves by accounting for charging/discharging with their efficiencies (η) and travel consumption ($c^{\mathrm{travel}}_{t,a}$) as the SoC update:

$$E_{t,a} = E^{\mathrm{Init}}_{t,a} + \sum_{i\in\Omega^{CS}} \eta\, A_{t,a,i}\, p^{\mathrm{CS}}_{a,i,t,\varphi} \Delta_{t,a,i} - c^{\mathrm{travel}}_{t,a}, \qquad \forall t, a. \quad (8)$$

$$E_{\min} \leq E_{t,a} \leq E_{\max}, \qquad \forall t, a. \quad (9)$$

$\Delta_{t,a,i}$ is the connection duration of EV a at station i during time t. In addition, to maintain feasible operation, Eq. (9) remains the SoC within the bounds $[E_{\min}, E_{\max}]$. Finally, we model travel energy as a uniform per-EV deduction during travel steps of each decision period:

$$c^{\mathrm{travel}}_{t,a} = \begin{cases} E^{\mathrm{tar}}/|\mathcal{T}^{\mathrm{trav}}_p|, & t \in \mathcal{T}^{\mathrm{trav}}_p, \\ 0, & \text{otherwise.} \end{cases} \quad (10)$$

where p is a period (it is defined as one hour), $\mathcal{T}^{\mathrm{trav}}_p$ is the set of travel steps within the period, and E^{tar} (kWh) is the travel-energy budget for one EV in that period, divided evenly across those travel steps. The optimization objective at each tracking step is to minimize the average tracking error at every EV charging station in the distribution network over the entire tracking horizon T.

$$\min \Big\{\sum_{t=1}^{T} \Big[\sum_{i\in\Omega^{CS}, \varphi\in\Phi} \beta^{CS}_i \big(p^{CS}_{i,t,\varphi} - P^{CS,ref}_{i,t,\varphi}\big)^2 / N^{CS} \Big] \Big\} \quad (11)$$

$$\text{s.t. Constraints: (1) – (6) and (9)}$$

where, β^{CS}_i is the coefficient for the tracking error calculations for charging stations, respectively. And, N^{CS} is to normalize the tracking errors for charging stations. The EV charging problem is modeled as a centralized convex optimization problem. The associated constraints can be categorized into global constraints and local constraints. Specifically, the global coupling is the shared feeder power-limit constraint applied at each time step, while the remaining constraints are local to each station/vehicle. Let $X \in \mathbb{R}^{T\times 6}$ stack the 6 station trajectories over time and denote the station net-power trajectories and $R \in \mathbb{R}^{T\times 6}$ the desired reference profiles. We minimize

$$\min_X \|X - R\|^2_F, \quad (12)$$

where $\|\cdot\|_F$ denotes the Frobenius norm. subject to the physical and operational constraints, station bounds and availability (zero power during travel steps), feeder capacity, state-of-charge dynamics. We pose EV scheduling as a centralized convex quadratic program that tracks station reference trajectories subject to linear feasibility constraints (bounds, feeder limits, availability) and per-EV SoC dynamics, yielding a globally optimal solution up to numerical tolerances [15].

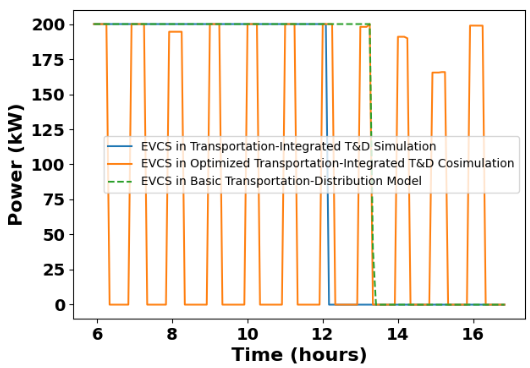

Fig. 3: Station-level power profiles of EVCSs 1–3 during peak demand under the three case studies.

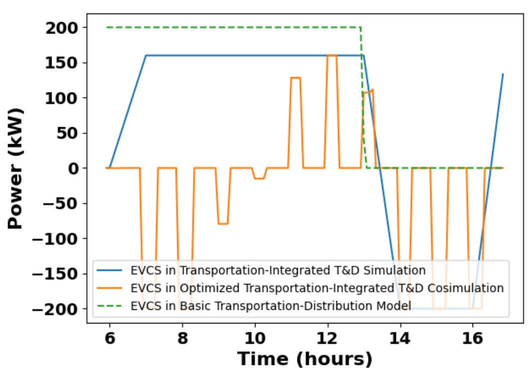

Fig. 4: Station-level power profiles of EVCS 4 during peak demand under the three case studies.

VI. Numerical Results

A. Simulation Setup

In the simulation, the power system is modeled with the IEEE 145-bus transmission network in GridPACK and the IEEE 123-bus three-phase unbalanced distribution feeder in GridLAB-D. The two simulators exchange data via HELICS at synchronized time steps. At each step, GridPACK publishes the complex voltage at Bus 2 as the distribution-substation boundary condition for GridLAB-D, and GridLAB-D computes the feeder response including the EV charging stations at the selected feeder nodes. EVs can be either charged or discharged at the charging stations, while each EV has an 85 kWh battery (by Tesla Model S [16]). The initial energy of each EV is uniformly sampled from $[0, 85]$ kWh as a neutral baseline to avoid bias toward a specific arrival state-of-charge pattern in the absence of site-specific charging data.

In the simulation, the charging/discharging performance at EVCSs is evaluated under three scenarios: a basic transportation–distribution model, a transportation-integrated T&D simulation, and our developed optimized transportation-integrated T&D cosimulation. To create a realistic EV charging case, charging demand profiles of EVCSs 5 and 6 are predicted from the transportation simulator, following time-varying 24-hour-schedules as shown in Fig. 2. EVCS 4 operates in charging and discharging modes, allowing discharging under peak conditions for scenarios 2 and 3. The distributed controller manages the power of EVCSs 4–6 dynamically in response to feeder loading throughout the day.

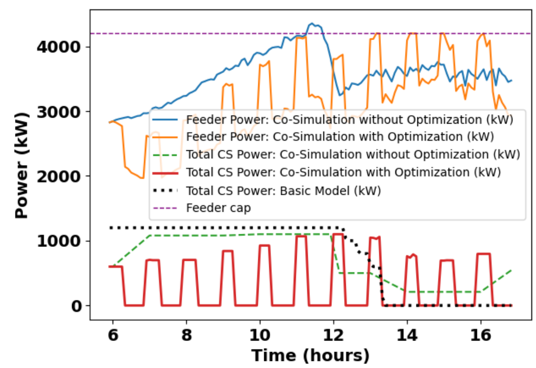

Fig. 5: Feeder vs. total CS powers during peak demand for three scenarios

B. Simulation Results

Table I shows substation voltage at 138 kV with symmetric phases $(0°, -120°, 120°)$ and EVCS voltages around 2.4–2.5 kV in the transportation-integrated T&D testbed. Each EVCS connects mainly to a single phase, with near-zero values on others. Minor deviations reflect load patterns, control, and feeder location. All voltages remain within limits, confirming compliant single-phase operation under coordinated charging.

Fig. 3 shows charging power at EVCS 1 (or EVCS 2/EVCS 3 that have the same behavior with EVCS 1). Specifically, as the green-dashed line shown in Fig. 3, under the transportation-distribution model, the stations are disconnected from the grid for a long period to shed the demand and prevent damaging the grid; however, as the blue line shown under the transportation-integrated T&D simulation, the controlled T&D co-simulation disconnects the stations approximately one hour earlier to protect the grid which demonstrating the impact of DER control on power grids within a T&D framework. Furthermore, the charging performance under our developed optimized transportation-integrated T&D testbed is shown as the orange line in Fig. 3. In addition to enabling travel schedules to increase the accuracy of the simulation, charging performance at the charging station replaces long plateaus with bounded, piecewise-constant bursts aligned to the 20-minute charge windows. It suppresses bursts near the feeder peak and defers them to lower-load shoulder periods, while allowing these three stations to be charged even during peak demand. This time-staggering reduces simultaneity

979-8-3315-8138-1

TABLE I: Voltage magnitudes (V) and phase angles (deg) at the substation and six EVCS nodes.

Node	$\lvert V_a \rvert$	$\angle V_a$ (°)	$\lvert V_b \rvert$	$\angle V_b$ (°)	$\lvert V_c \rvert$	$\angle V_c$ (°)
network_node	138000.00	0.00	138000.00	-120.00	138000.00	120.00
EVCS 6	2417.09	-2.68	0.00	0.00	0.00	0.00
EVCS 5	0.00	0.00	2491.71	-120.88	0.00	0.00
EVCS 4	0.00	0.00	0.00	0.00	2444.53	119.44
EVCS 3	2403.84	-3.36	0.00	0.00	0.00	0.00
EVCS 2	0.00	0.00	2448.40	-120.00	0.00	0.00
EVCS 1	0.00	0.00	0.00	0.00	2441.99	119.92

across EVCSs 1 to 3, delivers comparable total energy, and keeps their power within the $[0, 200]$ kW limits.

The charging performance of station 4 is shown in Fig. 4. During peak duration, the charging power remains non-negative near its $\sim 200\,\mathrm{kW}$ nameplate with no discharge in the baseline case. The second scenario enables V2G ,but in a concentrated block, the station is charging to satisfy SoC, and then executing a sustained discharge reaching about $-200\,\mathrm{kW}$ for more than two hours of this peak period. In contrast, our developed optimized case study spreads charge and discharge across the entire peak window, allocating smaller alternating pulses that share V2G contribution over time, reduce feeder demand, and still satisfy SoC and the V2G quota constraints.

Furthermore, Fig. 5 plots: (i) basic transportation–distribution model (black-dotted, total CS power), (ii) transportation-integrated T&D simulation (green-dashed total CS power; blue feeder power), and (iii) developed optimized transportation-integrated T&D co-simulation (red total CS power; orange feeder power). The feeder capacity is 4.2 MW (*purple-dashed line*). case study 1 and case study 2 have almost the same feeder demand as the blue curve. They both exceed the feeder limit at around 11 in the morning; as shown in Fig. 5, this forces the shutdown of EVCSs in the first case, although the second case study keeps EVCS 5 and EVCS 6 online to follow their traffic flow throughout the day. The optimized schedule in Fig. 5 shows its ability to reshape the total CS power demand into bounded time-staggered bursts and to shift charging from 11–13 h to shoulder hours; the feeder trace flattens in the peak window and remains at or below the maximum feeder capacity, achieving peak shaving without disconnecting the stations for a long period. This figure also shows that enabling travel schedules in the optimized case yields more accurate results than the other two cases, with the aggregate power of the six stations remaining lower from 6 to 11 until peak system demand.

VII. Conclusions

We presented a DER-centered T&D co-simulation testbed on HELICS that couples GridPACK (transmission) and GridLAB-D (distribution), integrates transportation and power domains, and demonstrates its application through a spatio-temporal EV charging strategy with an optimization layer that coordinates charging and discharging subject to feeder capacity, station bounds, and ramp limits. The simulation results show that the proposed coordinated charging strategy increases EV charging throughput while mitigating feeder peak loading and avoiding operational constraint violations. This strategy supports operational resilience under high EV penetration in a case study that includes DERs. As future work, the framework will be extended to multi-feeder systems and enhanced with dynamic analysis in GridPACK to better capture voltage–power interactions.

References

[1] A. Muhtadi, D. Pandit, N. Nguyen, and J. Mitra, “Distributed energy resources based microgrid: Review of architecture, control, and reliability,” *IEEE Trans. on Industry Applications*, vol. 57, no. 3, pp. 2223–2235, 2021.

[2] J. Y. Yong, W. S. Tan, M. Khorasany, and R. Razzaghi, “Electric vehicles destination charging: An overview of charging tariffs, business models and coordination strategies,” *Renewable and Sustainable Energy Reviews*, vol. 184, p. 113534, 2023.

[3] M. Abasi, J. Ebrahimi, and S. Besati, “Robust expansion planning of distribution network in presence of electric vehicles to improve economic parameters and reduce energy consumption,” *Engineering Reports*, vol. 7, no. 5, p. e70158, 2025.

[4] M. Paolone, T. Gaunt, X. Guillaud, M. Liserre, S. Meliopoulos, A. Monti, and C. Vournas, “Fundamentals of power systems modelling in the presence of converter-interfaced generation,” *Electric Power Systems Research*, vol. 189, p. 106811, 2020.

[5] U. Markovic, O. Stanojev, P. Aristidou, E. Vrettos, D. Callaway, and G. Hug, “Understanding small-signal stability of low-inertia systems,” *IEEE Trans. on Power Systems*, vol. 36, no. 5, pp. 3997–4017, 2021.

[6] M. Wang, R. Zhang, and T. Zang, “Spatio-temporal coordinated mobile electric vehicle charging in integrated transportation and distribution systems,” in *Proc. IEEE 99th Vehicular Technology Conference (VTC2024-Spring)*. Singapore, Singapore: IEEE, 2024, pp. 1–6.

[7] L. Zheng, Y. Cui, S. Jin, and Y. Chen, “High-performance computing-based open-source power transmission and distribution grid co-simulation,” *IEEE Trans. on Power Systems*, pp. 1–9, 2024.

[8] Pacific Northwest National Laboratory, “Gridlab-d: An open-source distribution system simulation and analysis tool,” 2013, available at http://www.gridlabd.org.

[9] B. J. Palmer and etc., “Gridpack™: A framework for developing power grid simulations on high-performance computing platforms,” *International Journal of High Performance Computing Applications*, vol. 30, no. 2, pp. 223–240, 2016, oSTI ID:1252842; DOE Contract AC05-76RL01830.

[10] A. Bharati and V. Ajjarapu, “Investigation of relevant distribution system representation with dg for voltage stability margin assessment,” *IEEE Trans. on Power Systems*, vol. 35, no. 3, pp. 2072–2081, 2020.

[11] M. A. I. Khan, A. Suresh, S. Paudyal, and S. Kamalasadan, “Decoupled and unified approaches for solving transmission and distribution co-simulations,” in *2019 North American Power Symposium (NAPS)*. IEEE, 2019, pp. 1–6.

[12] M. Rezvani, S. Mehraeen, J. Ramamurthy, and T. Field, “Dynamic interaction of distribution-connected der a with transmission system via co-simulation analysis,” *IEEE Trans. on Industrial Applications*, vol. 58, no. 2, pp. 1502–1511, 2022.

[13] HELICS Development Team, “Helics,” 2023, https://helics.org, Accessed: 2023-10-17.

[14] Y. Liu, R. Huang, W. Du, A. Singhal, and Z. Huang, “High-performance transmission and distribution co-simulation with 10,000+ inverter-based resources,” in *2022 IEEE Industry Applications Society Annual Meeting (IAS)*. IEEE, 2022, pp. 1–5.

[15] S. Boyd and L. Vandenberghe, *Convex Optimization*. Cambridge, U.K.: Cambridge University Press, 2004.

[16] https://www.tesla.com/models.

979-8-3315-8138-1